Prediction of pediatric unipolar depression using multiple neuromorphometric measurements: A pattern classification approach

Mon-Ju Wu[1], **Hanjing Emily Wu**[1], **Benson Mwangi**[1], **Marsal Sanches**[1], **Sudhakar Selvaraj**[1], **Giovana B. Zunta-Soares**[1], and **Jair C. Soares**[1]

[1]UT Center of Excellence on Mood Disorders, Department of Psychiatry and Behavioral Sciences, UT Houston Medical School, Houston, TX, USA.

Abstract

Background—Diagnosis of pediatric neuropsychiatric disorders such as unipolar depression is largely based on clinical judgment - without objective biomarkers to guide diagnostic process and subsequent therapeutic interventions. Neuroimaging studies have previously reported average *group-level* neuroanatomical differences between patients with pediatric unipolar depression and healthy controls. In the present study, we investigated the utility of multiple neuromorphometric indices in distinguishing pediatric unipolar depression patients from healthy controls at an individual subject level.

Methods—We acquired structural T_1-weighted scans from 25 pediatric unipolar depression patients and 26 demographically matched healthy controls. Multiple neuromorphometric indices such as cortical thickness, volume, and cortical folding patterns were obtained. A support vector machine pattern classification model was 'trained' to distinguish *individual* subjects with pediatric unipolar depression from healthy controls based on multiple neuromorphometric indices and model predictive validity (sensitivity and specificity) calculated.

Corresponding Author: Benson Mwangi, PhD, Department of Psychiatry & Behavioral Sciences, The University of Texas Health Science Center, 1941 East Road, Houston, TX, 77054, USA, Phone: +17134862624, Fax: +17134862553, benson.irungu@uth.tmc.edu.

Results—The model correctly identified 40 out of 51 subjects translating to 78.4% accuracy, 76.0 % sensitivity and 80.8 % specificity, chi-square p-value = 0.000049. Volumetric and cortical folding abnormalities in the right thalamus and right temporal pole respectively were most central in distinguishing individual patients with pediatric unipolar depression from healthy controls.

Conclusions—These findings provide evidence that a support vector machine pattern classification model using multiple neuromorphometric indices may qualify as diagnostic marker for pediatric unipolar depression. In addition, our results identified the most relevant neuromorphometric features in distinguishing PUD patients from healthy controls.

Keywords

Pediatric unipolar depression; neuroimaging; machine learning; support vector machine

Introduction

Major depressive disorder (MDD) or Unipolar Depression has a lifetime prevalence of 16.2 % in the adult population and affecting approximately 2.5 % of children and 8.3% of adolescents in the United States (Lewinsohn et al., 1994). Longitudinal studies have reported that a diagnosis of pediatric unipolar depression (PUD) is associated with an increased risk of recurrence during adulthood and that approximately 57.2 % of adult MDD cases may have started during childhood (Carballo et al., 2011) (Harrington et al., 1990, Rosso et al., 2005). In addition, PUD is associated with poor academic outcomes, impaired social functioning and elevated risks of substance abuse and other psychiatric comorbidities (Rao and Chen, 2009, Shad et al., 2012). These facts underscore the need to elucidate the pathophysiological mechanism of PUD and identify objective biomarkers able to assist in PUD diagnosis and guide treatment management.

In vivo neuroimaging studies have implicated multiple neuroanatomical structures in the pathophysiology of PUD. Notable findings include, reduced hippocampal (Caetano et al., 2007, MacMaster and Kusumakar, 2004, Rao et al., 2010), amygdala (Rosso, Cintron, 2005), striatum (Matsuo et al., 2008), caudate (Matsuo, Rosenberg, 2008, Shad, Muddasani, 2012) and increased left prefrontal cortex (Nolan et al., 2002) volumes. In addition, white matter abnormalities have also been reported in the corpus callosum (Caetano et al., 2008) and middle frontal gyrus (Ma et al., 2007). However, despite these multiple studies, significant limitations still exist. First, a majority of these studies utilized pre-defined anatomical regions-of-interest whilst recent studies have shown that neuroanatomical alterations in neuropsychiatric disorders involves multiple circuits as opposed to single anatomical regions – which underlines potential benefits of using whole brain neuroimaging scan data (Ecker et al., 2010, Good et al., 2002). Second, previous studies have not investigated the predictive utility (high specificity and sensitivity) of *in vivo* neuroimaging scans in distinguishing PUD patients from healthy controls but largely reported *average* group-level differences. Notably, multiple studies in other neuropsychiatric disorders – including adult unipolar depression and pediatric bipolar disorder have shown great potential of *in vivo* neuroimaging scans together with pattern classification or machine learning algorithms in distinguishing individual patients with neuropsychiatric disorders from healthy controls (Costafreda et al., 2009, Fu et al., 2008, Johnston et al., 2013, Mwangi et al., 2012,

Mwangi et al., 2014, Mwangi et al., 2013b, Nouretdinov et al., 2011, Orrù et al., 2012, Sun et al., 2009, Zeng et al., 2012). Third, previous PUD studies have largely utilized single neuromorphometric measurements (e.g. volume alone) whilst combining multiple measurements (e.g. anatomical volume and cortical thickness) may offer a complimentary view of brain structure which may further improve prediction accuracy (Ecker, Marquand, 2010).

In the present study, we set out to investigate the utility of multiple neuromorphometric measurements such as anatomical volume, cortical thickness, folding index, mean curvature, Gaussian curvature and intrinsic curvature index together with a machine learning algorithm in identifying individual subjects with PUD. These neuromorphometric measurements were extracted using Freesurfer software library (Fischl, 2012) and input into a support vector machine (SVM) (Vapnik, 1999) pattern classification model which was 'trained' to distinguish individual PUD patients from healthy controls. The model's ability to generalize from novel subjects' data was evaluated using a leave-one-out cross-validation (LOOCV) method which involved 'training' the model using all subjects but one - a process which was repeated until all subjects were left-out once. The 'left-out' subjects were used for estimating the model diagnostic accuracy, specificity, sensitivity, positive predictive value (PPV), negative predictive value (NPV), and an area under receiver operating characteristic curve (AUROC). A review of machine learning applications in psychiatric neuroimaging is given elsewhere (Ecker, Marquand, 2010, Mwangi, Ebmeier, 2012, Mwangi, Spiker, 2014, Mwangi, Tian, 2013b, Orrù, Pettersson-Yeo, 2012).

In summary, the main objective of this study was to examine the predictive validity of multiple neuromorphometric measurements acquired from T_1-weighted scans in distinguishing individual subjects with PUD from healthy controls.

Methods and Materials

Participants

This study was approved by the local Institutional review board (IRB) at The University of Texas Health Science Center at San Antonio. Study participants included 25 children and adolescents with DSM-IV diagnosis of unipolar depression and 26 age, gender, ethnicity, and pubertal status matched healthy controls with age ranging (8.5 – 17.5 years old). The diagnosis of unipolar depression in patients and the absence of Axis I pathology in controls was established through the administration of the Schedule for Affective Disorders and Schizophrenia for School-Age Children-Present and Lifetime version (K-SADS-PL) by a trained psychiatrist. Subjects were excluded if they met criteria for substance abuse or dependence in the 6 months that preceded their participation in the study. Healthy controls were excluded if they had any history of psychiatric disorders, including substance abuse or dependence, neurological disorders or a history of any Axis I psychiatric disorders in first degree relatives. Additional exclusion criteria were positive pregnancy test, neurological disorders, head injury with loss of consciousness, family history of hereditary neurologic disorders and presence of metallic objects in the body. Patient and healthy control groups did not differ significantly in terms of age, gender, ethnicity, years of education, pubertal development scale and social economic status. Conversely, the patient group differed

significantly on the child depression rating scale (CDRS) and the Hamilton depression rating scale (HDRS) as compared to Healthy controls and shown in Table 1.

Magnetic resonance imaging Protocol

Structural T_1-weighted MRI images were acquired using a 1.5 T Philips Gyroscan Intera scanner using a three-dimensional spoiled gradient recalled echo protocol with the following parameters. Repetition time (TR) = 24 ms, echo time (TE) = 5 ms, flip angle = 40°, field of view (FOV) = 24 cm, Slice thickness = 1 mm, voxel dimension = $1\times1\times1$ mm^3 and matrix size = 256×256. Scans were acquired by a trained MRI technologist and there were no consistent problems in scanning children and adolescents.

Image pre-processing

All T$_1$-weighted scans were visually inspected to rule out gross artefacts and input into the Freesurfer software library version 5.3.0 (Fischl, 2012, Fischl and Dale, 2000) for morphometric measurement and extraction. Briefly, the Freesurfer process involves the following steps. 1) Brain scan motion correction, non-uniform intensity normalization (Sled et al., 1998), non-brain tissue (e.g. skull and neck) removal and transformation of structural scans into the Talairach space. 2) Segmentation of subcortical white matter and gray matter anatomical volumes (Fischl et al., 2002). 3) Generation of volumetric and surface-based morphometric data (e.g. volume, cortical thickness). In the present study, the cerebral cortex was parcellated into 34 regions of interest (ROIs) per hemisphere based on an *a priori* atlas (Desikan et al., 2006). Notably, for each ROI, average cortical thickness (Fischl and Dale, 2000), cortical surface area, Gaussian curvature, mean curvature, Intrinsic Curvature index and folding index (Van Essen and Drury, 1997), and subcortical volume were extracted. Cortical thickness is measured as the distance between the pial surface and white-matter surface (Winkler et al., 2010) and reported to reflect degree of dendritic arborization (Ecker, Marquand, 2010, Huttenlocher, 1990) or altered myelination at the gray - white matter intersection (Ecker, Marquand, 2010). Gaussian curvature, mean curvature, Intrinsic Curvature index and folding index are geometric indices derived from the principal curvatures of the cortical surface (Pienaar et al., 2008, Ronan et al., 2011, Van Essen and Drury, 1997). Briefly, in geometry two principal curvatures (K_1 and K_2) of a surface are used to quantify folding of a 'regular surface' at every point within the surface (Gray et al., 1997). Gaussian curvature, mean curvature and intrinsic curvature index are all derived from the two principal curvatures as; Gaussian curvature = $K_1 \times K_2$,

mean curvature$=\frac{1}{2}(K_1+K_2)$. The intrinsic curvature index is computed as $\frac{1}{4\pi}\int\int k_3$, where $k_3 = |k_1 k_2|$ if $k_1 k_2 > 0$ or else $k_3 = 0$ (Van Essen and Drury, 1997). In contrast, the folding

index is computed as follows (Van Essen and Drury, 1997); $\frac{1}{4\pi}\int\int |k_1(|k_1| - |k_2|)|$. These geometric measurements are explored in detail in the supplementary materials and elsewhere (Van Essen and Drury, 1997). Notably though, high gaussian curvature, mean curvature and intrinsic curvature index represent a higher cortical folding, whist a high folding index implies higher directional cortical folding (e.g. axial). These metrics have been used previously to study aging trajectories (Wang et al., 2014) and neuropsychiatric disorders such as attention deficit hyperactivity disorder (ADHD) (Anderson et al., 2013, Colby et al.,

2012, Wolosin et al., 2009), Autism (Ecker, Marquand, 2010), Schizophrenia (Palaniyappan et al., 2011, Prasad et al., 2010), mild cognitive impairment (Cui et al., 2012) and Alzheimer's disease(Westman et al., 2013). Markedly, Freesurfer software library has reliably been used previously to extract and quantify neuromorphometric measurements in pediatric and adolescent studies (Almeida et al., 2010, Ecker, Marquand, 2010, McCauley et al., 2010, Wolosin, Richardson, 2009).

In summary, a total of 456 morphometric measurements covering the entire brain as shown in Table 2 were extracted per participant and used for subsequent analyses.

Data Analysis

Machine Learning—A support vector machine (SVM) (Vapnik, 1999) pattern classification model was implemented in Matlab (The Mathworks Inc.) using a SVM toolbox (Schwaighofer. 2001) and in house custom software as follows. First, given example training data (subjects' neuromorphometric measurements) and corresponding diagnostic targets (PUD +1 and healthy controls −1), the SVM algorithm was 'trained' to identify a boundary (hyperplane) that optimally separates patients from healthy controls. The identified boundary was later used during the 'testing' stage to categorize novel scan data as either PUD or healthy controls.

To test the model's generalization ability from novel data, 'training' and 'testing' datasets were separated using a leave-one-out cross-validation (LOOCV) (Johnston, Mwangi, 2013, Mwangi et al., 2013a) process. LOOCV involves training a model with all subjects but one whilst the 'left-out' subject is used for testing (Johnston, Mwangi, 2013). LOOCV process was repeated until all subjects were 'left-out' of the training process at-least once. LOOCV is typically used when the study sample is small to maximize the training sub-sample (Johnston, Mwangi, 2013, Mwangi, Tian, 2013b). A practical data partitioning alternative to LOOCV is the 'hold-out' or 'split-half' method but it requires a large number of observations (Theodoridis et al., 2010). The SVM training process required identification of three parameters. First, a kernel learning function for example; linear, polynomial and Gaussian (Bishop, 2006b, Vapnik, 1999). Second, a 'kernel function parameter' which allows the kernel learning function to calculate similarities between training examples (Bishop, 2006b, Mwangi, Ebmeier, 2012). Third, the model 'regularization parameter' which minimizes miss-classifications of novel subject data (Mwangi, Ebmeier, 2012, Orrù, Pettersson-Yeo, 2012). In the present study, we evaluated three kernel functions (linear, polynomial and Gaussian radial basis function). Gaussian radial basis function kernel and regularization parameters were selected using a *grid-search* process using training data only.

However, the number of predictor variables (neuromorphometric measurements) greatly exceeded the sample size (number of subjects), resulting in a common problem in machine learning known as the *curse-of-dimensionality* or *small-n-large-p problem* (Bishop, 2006a). This problem requires a feature reduction or feature subset selection step to remove redundant predictor variables as shown in previous neuroimaging machine learning studies (De Martino et al., 2008, Mwangi, Hasan, 2013a, Mwangi, Tian, 2013b). In the present study though, we first evaluated the predictive validity (high sensitivity and specificity) of the model without performing feature reduction. Secondly, we evaluated the utility of two

feature reduction techniques namely; a univariate t-test filter and a SVM recursive feature elimination (RFE) wrapper in enhancing the predictive validity of the model. A review and introduction of feature reduction techniques in neuroimaging is given elsewhere (Mwangi, Tian, 2013b). Importantly, in the univariate t-test filter feature reduction step, a two-sample univariate t-test was performed between features from both groups and a significance p-value returned whilst SVM was used to evaluate the p-value threshold leading to best predictive accuracy. This feature reduction approach (univariate t-test filter) has previously been used elsewhere in psychiatric neuroimaging studies (Craddock et al., 2009, De Martino, Valente, 2008, Mwangi, Ebmeier, 2012, Mwangi, Tian, 2013b). In the present study, feature reduction was performed using training data only to avoid *double-dipping* (Mwangi, Tian, 2013b) as shown in Figure 1.

This pattern classification framework was initially evaluated using *individual* neuromorphometric measurements (e.g. cortical thickness only) and subsequently using combined neuromorphometric measurements (e.g. volume, cortical thickness, folding index, mean curvature, Gaussian curvature and intrinsic curvature index). In the latter case, all neuromorphometric measurements were combined by concatenation and input into the SVM model as shown in Figure 1. Model accuracy, specificity, sensitivity, positive predictive value, negative predictive value and area under receiver operating characteristic curve were calculated. These parameters are used to *objectively* evaluate predictive validity of pattern classification or machine learning models in predicting individual subjects and are explored in detail elsewhere (Mwangi, Ebmeier, 2012, Orrù, Pettersson-Yeo, 2012). Lastly, neuromorphometric features most relevant in distinguishing individual subjects with PUD from healthy controls were identified by calculating the number of times a feature was identified as relevant in all LOOCV iterations as shown in Figure 2.

Results

Table 1 summarizes subjects' demographic and clinical details. Patient and Healthy control groups did not differ significantly in terms of age, gender, ethnicity, years of education and pubertal development scale. The SVM model trained using all neuromorphometric measurements performed best with accuracy = 78.4%, sensitivity =76%, specificity =80.8% and area under receiver operating characteristic curve = 0.784 as shown in Figure 3. A detailed table of individual subjects predictions is given in table S1 of supplementary materials. Performance of the model 'trained' using individual neuromorphometric features (e.g. volume only) against multiple features (e.g. volume plus cortical thickness) is shown in Table 2. The SVM model trained using a 2nd order polynomial kernel function returned the best accuracy 78.4% whilst other kernel functions returned a moderate to poor accuracy (linear = 72.6%, Gaussian radial basis function = 47.0%). The SVM model trained without feature reduction performed poorly (accuracy= 52.9%, chi-squre p=0.69). Notably, the SVM model trained using a – recursive feature elimination (RFE) feature reduction process performed only marginally (accuracy =58%, chi-square p=0.21) whilst the model using a *univariate* filtering feature reduction process performed best with 78.4% accuracy. There were no significant demographic differences between correctly classified (true positives) and miss-classified patient groups (false negatives) (age of two group independent sample t-test p=0.3, gender of chi-square p=0.5, number of episodes of two group independent

sample t-test p=0.5, length of illness of two group independent sample t-test p=0.5, number of comorbidities of two group independent sample t-test p=0.1, Petersen pubertal score of two group independent sample t-test p=0.67). Similarly, no significant differences in clinical variables were identified between correctly classified and miss-classified patient groups (child depression rating scale of two group independent sample t-test p=0.1 and Hamilton depression rating scale of two group independent sample t-test p=0.86).

The model identified the right thalamus volume and right temporal pole Gaussian curvature, mean curvature and intrinsic Curvature index as most relevant in distinguishing PUD patients from healthy controls as shown in Figure 2 (a). A *post-hoc* independent two sample t-test was used to investigate the null hypothesis of no volumetric difference between PUD patients and healthy controls in the right thalamus as shown in Figure 4(a). A similar calculation was repeated for Gaussian curvature, mean curvature and intrinsic Curvature index as shown in Figures 4(b–d). The null hypothesis was rejected and determined that all four neuromorphometric features differed significantly between groups.

Discussion

In the present study, we report accurate predictions of individual PUD patients using neuromorphometric measurements obtained from structural T_1-weighted scans. Markedly, combination of multiple neuromorphometric measurements (e.g. volume and cortical thickness) resulted to higher prediction accuracy as compared to individual measurements indicating these multiple measurements may offer complimentary information on brain structure as recently reported in other studies (Ecker, Marquand, 2010, Peng et al., 2013). We report a prediction accuracy, specificity and sensitivity comparable to other machine learning studies in neuropsychiatry which have reported predictive accuracies ranging from (70–90%) (Ecker, Marquand, 2010, Fu, Mourao-Miranda, 2008, Mwangi, Ebmeier, 2012, Peng, Lin, 2013). In the present study, the right thalamus and right temporal pole were most relevant in distinguishing PUD patients from healthy controls indicating altered neural systems in these regions. We believe, this is a significant advance given that previous studies have largely reported *region-of-interest* or whole-brain *average* group-level differences between PUD patient groups and healthy controls. In addition, we highlight notable benefits of using a pattern classification approach. First, pattern classification models return a diagnostic decision value at an *individual* subject level whist conventional univariate statistical methods provide *group-level* differences only (Bray et al., 2009). Notably, being able to identify patients at an individual subject level may potentially allow therapeutic interventions tailored to individual subjects (Mwangi, Ebmeier, 2012). Second, pattern classification models utilize a robust cross-validation process to evaluate generalization ability from 'novel' subject data a process which allows an investigator to make objective conclusions (Johnston, Mwangi, 2013).

The thalamus is a critical component of the heavily interconnected limbic-cortical-striatal-pallidal-thalamic circuitry which is involved in reward learning and emotion processing and has been reported to be dysfunctional in mood disorders (Konarski et al., 2008, Price and Drevets, 2012). Previous neuroimaging studies have reported volumetric reductions in the thalamus in adult patients with major depression, obsessive compulsive disorder and bipolar

disorders (Atmaca et al., 2007, Gilbert et al., 2000, Kim et al., 2008, Rimol et al., 2010). Notably, a recent functional neuroimaging study reported an increased right lateralized amygdala-thalamic activation during a face processing task in clinically depressed children (Gaffrey et al., 2013). In the present study, both the Gaussian curvature and the intrinsic curvature index of the right temporal pole were the second most relevant neuromorphometric measurements in predicting PUD from healthy controls. The temporal pole is the anterior-most portion of the temporal lobes and considered part of an extended limbic system due to its location lateral to amygdala, posterior to orbital frontal cortex and heavily interconnected to the limbic and paralimbic regions (Olson et al., 2007). Markedly, previous functional imaging studies have implicated the temporal pole in socio-emotional processing tasks (Olson, Plotzker, 2007). We observed significantly higher temporal pole mean, Gaussian and intrinsic curvature indices in PUD patients as compared to healthy controls indicating a higher degree of cortical folding in patients as compared to healthy controls. Most notably, studies characterizing developmental cortical folding patterns have reported that brain curvature measurements (e.g. Gaussian curvature) decline from early childhood to adulthood (Pienaar, Fischl, 2008).

Potential limitations of this study should be noted. First, twelve patients were currently or previously under psychotropic medications which reflects standard clinical practice. Individual subjects' medication status are included in the supplementary materials table S1. However, There was no interaction between SVM model predictions and medication status (chi-square p=0.2). Second, a substantial portion of our PUD sample also met criteria for co-occurring anxiety disorders which limits our ability to make definite conclusions that observed abnormalities are limited to PUD only and not related to these comorbidities. Notably, a high co-occurrence of anxiety disorders and major depression has extensively been reported in previous studies (Brady and Kendall, 1992, Brown et al., 2001). Third, our sample size was relatively small and results will need to be replicated in a larger sample. In addition, the accuracy reported using cortical surface area was 17.65% and below chance ($< 50\%$). Notably, this is known as the 'anti-learning' phenomenon in the machine learning literature (Jacob and Vert, 2008, Kowalczyk, 2007, Kowalczyk and Chapelle, 2005, Roadknight et al., 2012) and still not well understood. The presence of this phenomenon in surface area and not in other morphometric measurements was unclear to us and warrants further investigation in the future in the context of machine learning literature. However, when cortical surface area was combined with other features – this phenomenon was not present. Notably, this may be in line with (Guyon and Elisseeff, 2003) argument that a feature by itself may not be relevant to a multivariate model but when combined with others it becomes relevant. Our study did not assess the utility of this technique in distinguishing PUD patients from other neurodevelopmental or neuropsychiatric disorders (e.g. bipolar disorders and anxiety disorders) but work is ongoing in our group to investigate this hypothesis. Lastly, identified anatomical regions largely in the right hemisphere as most relevant in distinguishing PUD patients from Healthy controls – a finding which was unanticipated and warrants further investigation in future studies.

In summary, we present a novel pattern classification framework able to predict pediatric patients with unipolar depression from healthy with a high diagnostic accuracy. Importantly,

further work is needed to replicate these findings before they are considered for use in clinical practice.

However, if such a technique as described in this study is available in psychiatric clinical practice, this would allow timely and targeted therapeutic interventions and ultimately reap the benefits of individualized or personalized medicine.

Supplementary Material

Refer to Web version on PubMed Central for supplementary material.

Acknowledgments

References

Almeida LG, Ricardo-Garcell J, Prado H, Barajas L, Fernández-Bouzas A, Ávila D, et al. Reduced right frontal cortical thickness in children, adolescents and adults with ADHD and its correlation to clinical variables: a cross-sectional study. Journal of psychiatric research. 2010; 44:1214–1223. [PubMed: 20510424]

Anderson A, Douglas PK, Kerr WT, Haynes VS, Yuille AL, Xie J, et al. Non-negative matrix factorization of multimodal MRI, fMRI and phenotypic data reveals differential changes in default mode subnetworks in ADHD. NeuroImage. 2013

Atmaca M, Yildirim H, Ozdemir H, Tezcan E, Kursad Poyraz A. Volumetric MRI study of key brain regions implicated in obsessive–compulsive disorder. Progress in neuro-psychopharmacology and Biological Psychiatry. 2007; 31:46–52. [PubMed: 16859819]

Bishop, CM. Pattern recognition and machine learning. New York: springer; 2006a.

Bishop, CM. Pattern Recognition and Machine Learning. Springer; 2006b.

Brady EU, Kendall PC. Comorbidity of anxiety and depression in children and adolescents. Psychological Bulletin. 1992; 111:244. [PubMed: 1557475]

Bray S, Chang C, Hoeft F. Applications of multivariate pattern classification analyses in developmental neuroimaging of healthy and clinical populations. Front Human Neurosci. 2009:3.

Brown TA, Campbell LA, Lehman CL, Grisham JR, Mancill RB. Current and lifetime comorbidity of theDSM-IV anxiety and mood disorders in a large clinical sample. Journal of Abnormal Psychology. 2001; 110:585. [PubMed: 11727948]

Caetano SC, Fonseca M, Hatch JP, Olvera RL, Nicoletti M, Hunter K, et al. Medial temporal lobe abnormalities in pediatric unipolar depression. Neuroscience letters. 2007; 427:142–147. [PubMed: 17949901]

Caetano SC, Silveira CM, Kaur S, Nicoletti M, Hatch JP, Brambilla P, et al. Abnormal corpus callosum myelination in pediatric bipolar patients. Journal of affective disorders. 2008; 108:297–301. [PubMed: 18037496]

Carballo JJ, Muñoz-Lorenzo L, Blasco-Fontecilla H, Lopez-Castroman J, García-Nieto R, Dervic K, et al. Continuity of depressive disorders from childhood and adolescence to adulthood: a naturalistic study in community mental health centers. The primary care companion to CNS disorders. 2011:13.

Colby JB, Rudie JD, Brown JA, Douglas PK, Cohen MS, Shehzad Z. Insights into multimodal imaging classification of ADHD. Frontiers in systems neuroscience. 2012:6. [PubMed: 22438838]

Costafreda SG, Chu C, Ashburner J, Fu CH. Prognostic and diagnostic potential of the structural neuroanatomy of depression. PLoS One. 2009; 4:e6353. [PubMed: 19633718]

Craddock RC, Holtzheimer PE, Hu XP, Mayberg HS. Disease state prediction from resting state functional connectivity. Magnetic resonance in Medicine. 2009; 62:1619–1628. [PubMed: 19859933]

Cui Y, Sachdev PS, Lipnicki DM, Jin JS, Luo S, Zhu W, et al. Predicting the development of mild cognitive impairment: a new use of pattern recognition. Neuroimage. 2012; 60:894–901. [PubMed: 22289804]

De Martino F, Valente G, Staeren N, Ashburner J, Goebel R, Formisano E. Combining multivariate voxel selection and support vector machines for mapping and classification of fMRI spatial patterns. Neuroimage. 2008; 43:44–58. [PubMed: 18672070]

Desikan RS, Ségonne F, Fischl B, Quinn BT, Dickerson BC, Blacker D, et al. An automated labeling system for subdividing the human cerebral cortex on MRI scans into gyral based regions of interest. Neuroimage. 2006; 31:968–980. [PubMed: 16530430]

Ecker C, Marquand A, Mourão-Miranda J, Johnston P, Daly EM, Brammer MJ, et al. Describing the brain in autism in five dimensions—magnetic resonance imaging-assisted diagnosis of autism spectrum disorder using a multiparameter classification approach. The Journal of Neuroscience. 2010; 30:10612–10623. [PubMed: 20702694]

Fischl B. FreeSurfer. Neuroimage. 2012; 62:774–781. [PubMed: 22248573]

Fischl B, Dale AM. Measuring the thickness of the human cerebral cortex from magnetic resonance images. Proceedings of the National Academy of Sciences. 2000; 97:11050–11055.

Fischl B, Salat DH, Busa E, Albert M, Dieterich M, Haselgrove C, et al. Whole brain segmentation: automated labeling of neuroanatomical structures in the human brain. Neuron. 2002; 33:341–355. [PubMed: 11832223]

Fu CH, Mourao-Miranda J, Costafreda SG, Khanna A, Marquand AF, Williams SC, et al. Pattern classification of sad facial processing: toward the development of neurobiological markers in depression. Biological psychiatry. 2008; 63:656–662. [PubMed: 17949689]

Gaffrey MS, Barch DM, Singer J, Shenoy R, Luby JL. Disrupted amygdala reactivity in depressed 4-to 6-year-old children. Journal of the American Academy of Child and Adolescent Psychiatry. 2013; 52:737–746. [PubMed: 23800487]

Gilbert AR, Moore GJ, Keshavan MS, Paulson LAD, Narula V, Mac Master FP, et al. Decrease in thalamic volumes of pediatric patients with obsessive-compulsive disorder who are taking paroxetine. Archives of General Psychiatry. 2000; 57:449–456. [PubMed: 10807485]

Good, CD.; Johnsrude, IS.; Ashburner, J.; Henson, RN.; Fristen, K.; Frackowiak, RS. Biomedical Imaging, 2002 5th IEEE EMBS International Summer School on. IEEE; 2002. A voxel-based morphometric study of ageing in 465 normal adult human brains; p. 16

Gray, A.; Abbena, E.; Salamon, S. Modern differential geometry of curves and surfaces with Mathematica. Boca Raton FL: 1997. p. 373-380.

Guyon I, Elisseeff A. An introduction to variable and feature selection. The Journal of Machine Learning Research. 2003; 3:1157–1182.

Harrington R, Fudge H, Rutter M, Pickles A, Hill J. Adult outcomes of childhood and adolescent depression: I. Psychiatric status. Archives of General Psychiatry. 1990; 47:465–473. [PubMed: 2184797]

Huttenlocher PR. Morphometric study of human cerebral cortex development. Neuropsychologia. 1990; 28:517–527. [PubMed: 2203993]

Jacob L, Vert J-P. Protein-ligand interaction prediction: an improved chemogenomics approach. Bioinformatics. 2008; 24:2149–2156. [PubMed: 18676415]

Johnston B, Mwangi B, Matthews K, Coghill D, Steele J. Predictive classification of individual magnetic resonance imaging scans from children and adolescents. European child & adolescent psychiatry. 2013; 22:733–744. [PubMed: 22930323]

Kim MJ, Hamilton JP, Gotlib IH. Reduced caudate gray matter volume in women with major depressive disorder. Psychiatry Research: Neuroimaging. 2008; 164:114–122.

Konarski JZ, McIntyre RS, Kennedy SH, Rafi-Tari S, Soczynska JK, Ketter TA. Volumetric neuroimaging investigations in mood disorders: bipolar disorder versus major depressive disorder. Bipolar disorders. 2008; 10:1–37. [PubMed: 18199239]

Kowalczyk, A. Knowledge Discovery in Databases: PKDD 2007. Springer; 2007. Classification of anti-learnable biological and synthetic data; p. 176-187.

Kowalczyk, A.; Chapelle, O. Algorithmic Learning Theory. Springer; 2005. An analysis of the anti-learning phenomenon for the class symmetric polyhedron; p. 78-91.

Lewinsohn PM, Clarke GN, Seeley JR, Rohde P. Major depression in community adolescents: age at onset, episode duration, and time to recurrence. Journal of the American Academy of Child & Adolescent Psychiatry. 1994; 33:809–818. [PubMed: 7598758]

Ma N, Li L, Shu N, Liu J, Gong G, He Z, et al. White matter abnormalities in first-episode, treatment-naive young adults with major depressive disorder. American Journal of Psychiatry. 2007; 164:823–826. [PubMed: 17475743]

MacMaster FP, Kusumakar V. Hippocampal volume in early onset depression. BMC medicine. 2004; 2:2. [PubMed: 14969587]

Matsuo K, Rosenberg DR, Easter PC, MacMaster FP, Chen H-H, Nicoletti M, et al. Striatal volume abnormalities in treatment-naive patients diagnosed with pediatric major depressive disorder. Journal of child and adolescent psychopharmacology. 2008; 18:121–131. [PubMed: 18439110]

McCauley SR, Wilde EA, Merkley TL, Schnelle KP, Bigler ED, Hunter JV, et al. Patterns of cortical thinning in relation to event-based prospective memory performance three months after moderate to severe traumatic brain injury in children. Developmental neuropsychology. 2010; 35:318–332. [PubMed: 20446135]

Mwangi B, Ebmeier KP, Matthews K, Steele JD. Multi-centre diagnostic classification of individual structural neuroimaging scans from patients with major depressive disorder. Brain. 2012; 135:1508–1521. [PubMed: 22544901]

Mwangi B, Hasan KM, Soares JC. Prediction of individual subject's age across the human lifespan using diffusion tensor imaging: A machine learning approach. NeuroImage. 2013a; 75:58–67. [PubMed: 23501046]

Mwangi B, Spiker D, Zunta-Soares GB, Soares JC. Prediction of pediatric bipolar disorder using neuroanatomical signatures of the amygdala. Bipolar Disorders. 2014 n/a-n/a.

Mwangi B, Tian TS, Soares JC. A Review of Feature Reduction Techniques in Neuroimaging. Neuroinformatics. 2013b:1–16. [PubMed: 23224666]

Nolan CL, Moore GJ, Madden R, Farchione T, Bartoi M, Lorch E, et al. Prefrontal cortical volume in childhood-onset major depression: preliminary findings. Archives of general psychiatry. 2002; 59:173–179. [PubMed: 11825139]

Nouretdinov I, Costafreda SG, Gammerman A, Chervonenkis A, Vovk V, Vapnik V, et al. Machine learning classification with confidence: application of transductive conformal predictors to MRI-based diagnostic and prognostic markers in depression. Neuroimage. 2011; 56:809–813. [PubMed: 20483379]

Olson IR, Plotzker A, Ezzyat Y. The enigmatic temporal pole: a review of findings on social and emotional processing. Brain. 2007; 130:1718–1731. [PubMed: 17392317]

Orrù G, Pettersson-Yeo W, Marquand AF, Sartori G, Mechelli A. Using support vector machine to identify imaging biomarkers of neurological and psychiatric disease: a critical review. Neuroscience & Biobehavioral Reviews. 2012; 36:1140–1152. [PubMed: 22305994]

Palaniyappan L, Mallikarjun P, Joseph V, White TP, Liddle PF. Folding of the prefrontal cortex in schizophrenia: regional differences in gyrification. Biological psychiatry. 2011; 69:974–979. [PubMed: 21257157]

Peng X, Lin P, Zhang T, Wang J. Extreme Learning Machine-Based Classification of ADHD Using Brain Structural MRI Data. PloS one. 2013; 8:e79476. [PubMed: 24260229]

Pienaar R, Fischl B, Caviness V, Makris N, Grant PE. A methodology for analyzing curvature in the developing brain from preterm to adult. International journal of imaging systems and technology. 2008; 18:42–68. [PubMed: 19936261]

Prasad KM, Goradia D, Eack S, Rajagopalan M, Nutche J, Magge T, et al. Cortical surface characteristics among offspring of schizophrenia subjects. Schizophrenia research. 2010; 116:143–151. [PubMed: 19962858]

Price JL, Drevets WC. Neural circuits underlying the pathophysiology of mood disorders. Trends in cognitive sciences. 2012; 16:61–71. [PubMed: 22197477]

Rao U, Chen L-A. Characteristics, correlates, and outcomes of childhood and adolescent depressive disorders. Dialogues in clinical neuroscience. 2009; 11:45. [PubMed: 19432387]

Rao U, Chen L-A, Bidesi AS, Shad MU, Thomas MA, Hammen CL. Hippocampal changes associated with early-life adversity and vulnerability to depression. Biological psychiatry. 2010; 67:357–364. [PubMed: 20015483]

Rimol LM, Hartberg CB, Nesvåg R, Fennema-Notestine C, Hagler DJ Jr, Pung CJ, et al. Cortical thickness and subcortical volumes in schizophrenia and bipolar disorder. Biological psychiatry. 2010; 68:41–50. [PubMed: 20609836]

Roadknight, C.; Aickelin, U.; Qiu, G.; Scholefield, J.; Durrant, L. Systems, Man, and Cybernetics (SMC), 2012 IEEE International Conference on. IEEE; 2012. Supervised learning and anti-learning of colorectal cancer classes and survival rates from cellular biology parameters; p. 797-802.

Ronan L, Pienaar R, Williams G, Bullmore E, Crow TJ, Roberts N, et al. Intrinsic curvature: a marker of millimeter-scale tangential cortico-cortical connectivity? International journal of neural systems. 2011; 21:351–366. [PubMed: 21956929]

Rosso IM, Cintron CM, Steingard RJ, Renshaw PF, Young AD, Yurgelun-Todd DA. Amygdala and hippocampus volumes in pediatric major depression. Biological psychiatry. 2005; 57:21–26. [PubMed: 15607296]

Schwaighofer A. SVM Toolbox. 2001

Shad MU, Muddasani S, Rao U. Gray matter differences between healthy and depressed adolescents: a voxel-based morphometry study. Journal of child and adolescent psychopharmacology. 2012; 22:190–197. [PubMed: 22537357]

Sled JG, Zijdenbos AP, Evans AC. A nonparametric method for automatic correction of intensity nonuniformity in MRI data. Medical Imaging, IEEE Transactions on. 1998; 17:87–97.

Sun D, van Erp TG, Thompson PM, Bearden CE, Daley M, Kushan L, et al. Elucidating a magnetic resonance imaging-based neuroanatomic biomarker for psychosis: classification analysis using probabilistic brain atlas and machine learning algorithms. Biological psychiatry. 2009; 66:1055–1060. [PubMed: 19729150]

Theodoridis, S.; Pikrakis, A.; Koutroumbas, K.; Cavouras, D. Academic Press; 2010. Introduction to Pattern Recognition: A Matlab Approach: A Matlab Approach.

Van Essen D, Drury H. Structural and functional analyses of human cerebral cortex using a surface-based atlas. The Journal of Neuroscience. 1997; 17:7079–7102. [PubMed: 9278543]

Vapnik VN. An overview of statistical learning theory. Neural Networks, IEEE Transactions on. 1999; 10:988–999.

Wang J, Li W, Miao W, Dai D, Hua J, He H. Age estimation using cortical surface pattern combining thickness with curvatures. Medical & biological engineering & computing. 2014; 52:331–341. [PubMed: 24395657]

Westman E, Aguilar C, Muehlboeck J-S, Simmons A. Regional magnetic resonance imaging measures for multivariate analysis in Alzheimer's disease and mild cognitive impairment. Brain topography. 2013; 26:9–23. [PubMed: 22890700]

Winkler AM, Kochunov P, Blangero J, Almasy L, Zilles K, Fox PT, et al. Cortical thickness or grey matter volume? The importance of selecting the phenotype for imaging genetics studies. Neuroimage. 2010; 53:1135–1146. [PubMed: 20006715]

Wolosin SM, Richardson ME, Hennessey JG, Denckla MB, Mostofsky SH. Abnormal cerebral cortex structure in children with ADHD. Human brain mapping. 2009; 30:175–184. [PubMed: 17985349]

Zeng L-L, Shen H, Liu L, Wang L, Li B, Fang P, et al. Identifying major depression using whole-brain functional connectivity: a multivariate pattern analysis. Brain. 2012; 135:1498–14507. [PubMed: 22418737]

Highlights

- Multiple neuromorphometric features are quantified using T_1-weighted scans.

- Support vector machines predict pediatric unipolar depression (PUD) patients.

- The prediction of PUD patients is performed at an individual subject level.

- Anatomical regions most relevant in predicting PUD patients are identified.
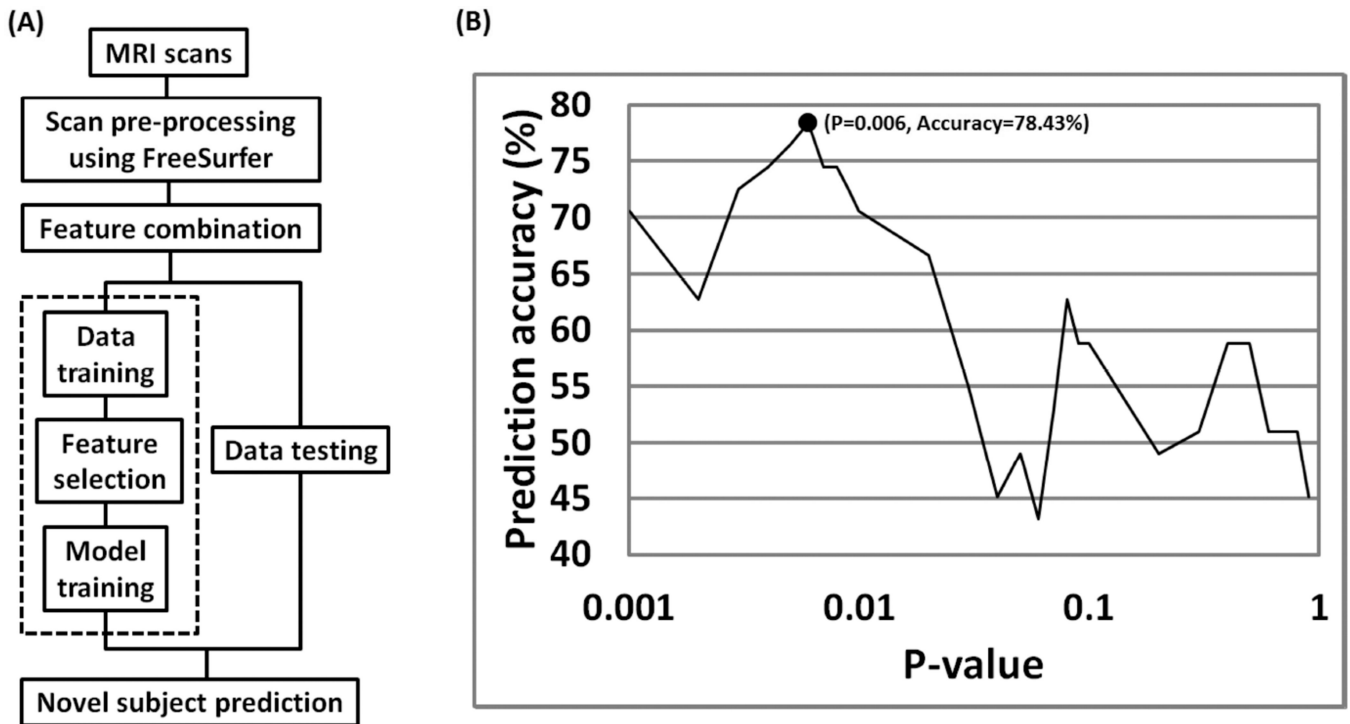
Figure 1.
Flow diagram illustrating SVM model training (using 2nd order polynomial kernel), feature subset selection and model testing process. A) Multiple neuromorphometric measurements were extracted using Freesurfer and combined through concatenation. B) Relevant features were identified using a univariate t-test filter on training data only using a nested leave-one-out cross-validation process. In a single feature selection iteration (dashed line in Figure 1a) – the model selected most optimal t-test p-value = 0.006) as shown in Figure 1b.
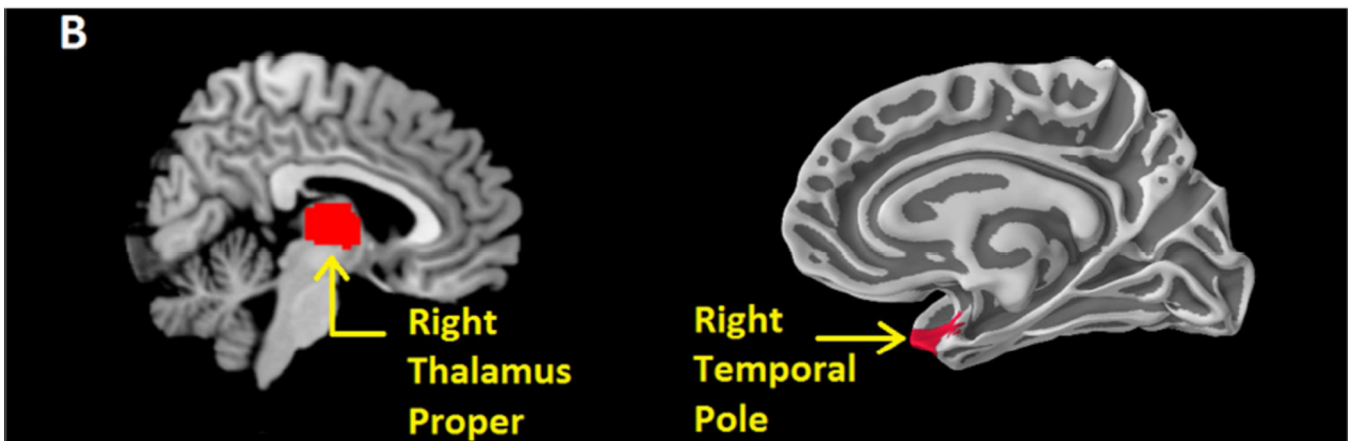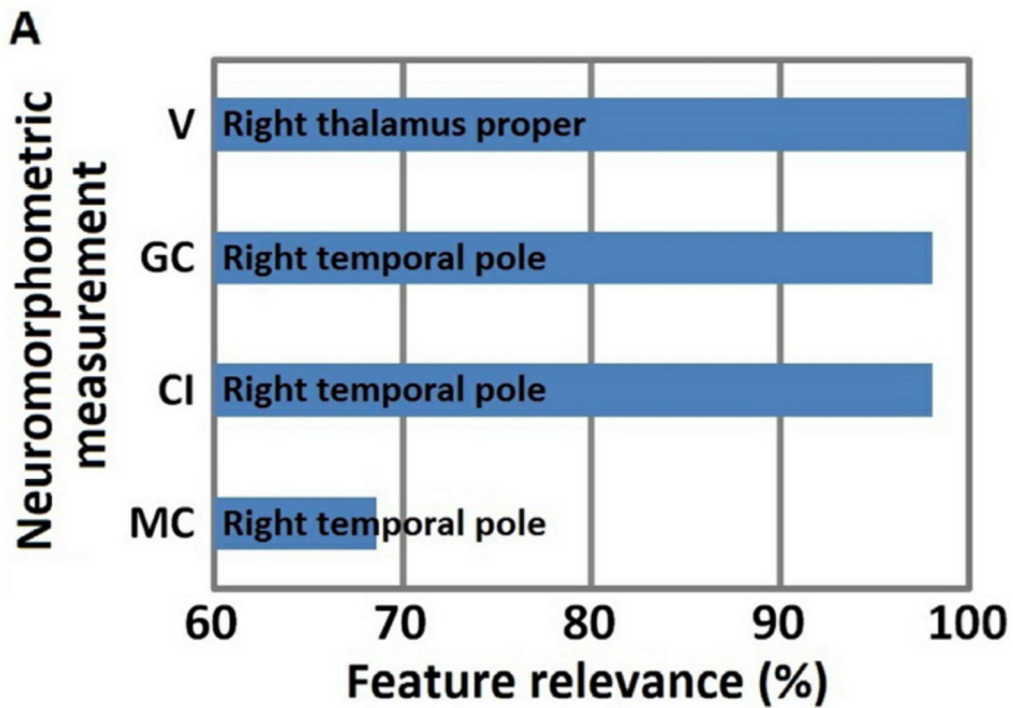
Figure 2.
A) Most relevant anatomical regions identified by the model. Right thalamus volume (V) was identified in all LOOCV iterations (100%) followed by right temporal pole Gaussian curvature (GC), Intrinsic Curvature index (CI) and mean curvature (MC). B) Anatomical regions most relevant in distinguishing PUD patients and healthy controls. Right thalamus proper and right temporal pole.
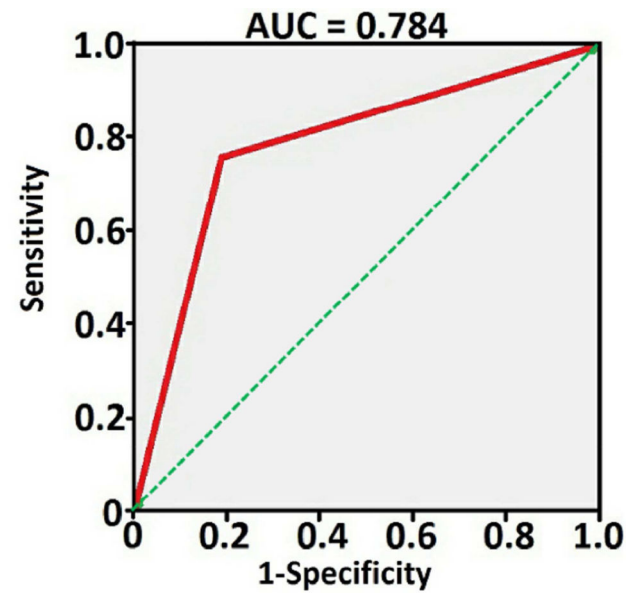
Figure 3.
Model confusion matrix and receiver operating characteristic curve. Model accuracy = 78.4 %, sensitivity = 76 %, specificity = 80.8 %, positive predictive value = 79.2 %, negative predictive value = 77.8%, and the chi-square p-value = 0.000049. The prediction was performed using standard SVM with 2nd order polynomial.
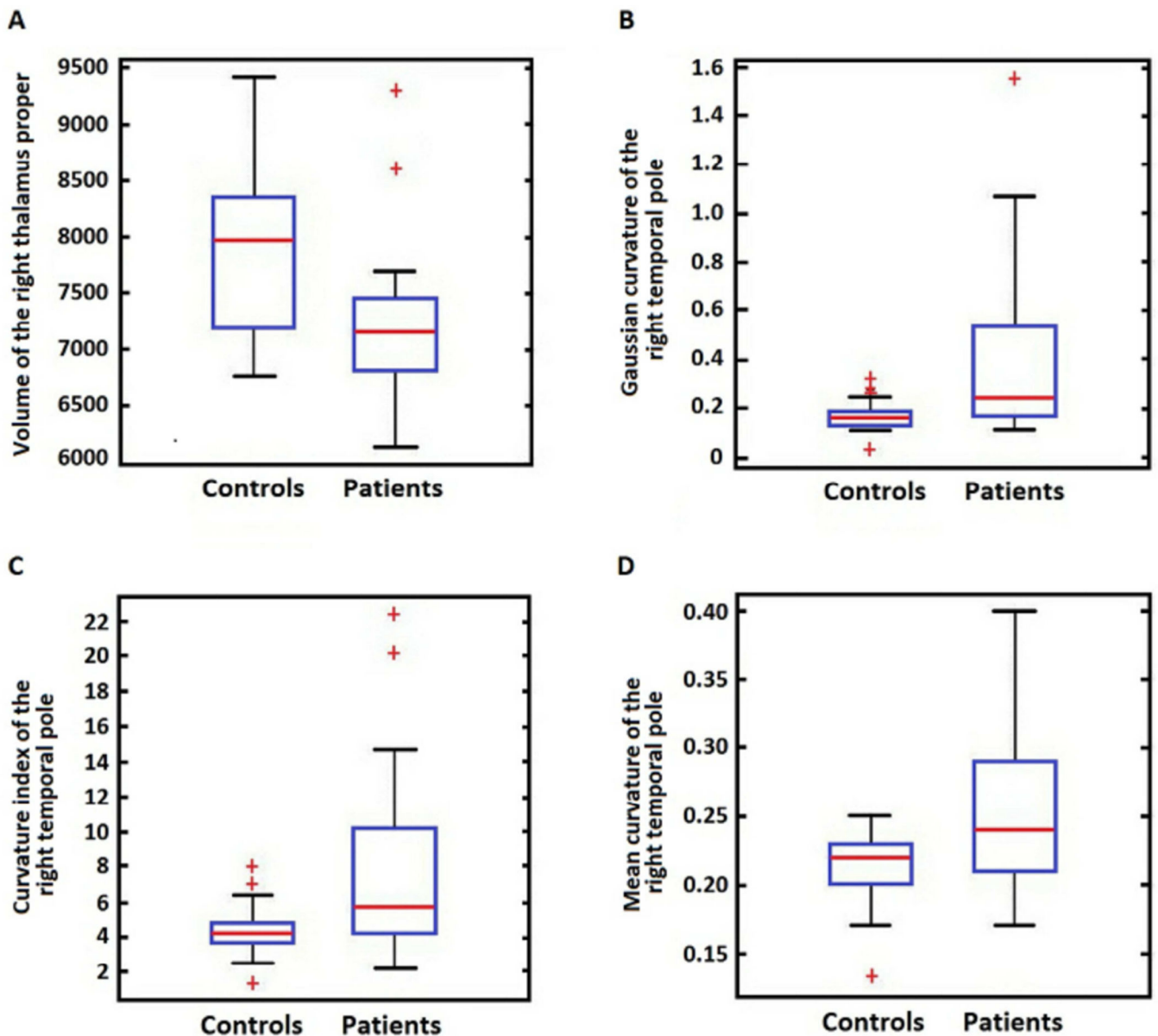
Figure 4.
A) Box plot showing significantly smaller right thalamus proper in PUD patients (two group independent sample t-test p=0.0005. B) Box plot showing significantly higher Gaussian curvature in PUD patients (two group independent sample t-test p=0.0026). C) Box plot showing significantly higher mean curvature (two group independent sample t-test p=0.005) in PUD patients D) Box plot showing significantly higher intrinsic curvature index in PUD patients (two group independent sample t-test p=0.0022).

Table 1

Demographics

	PUD mean(SD)	Healthy controls mean(SD)	P-value
Age(years)	13.07(2.55)	13.18(2.62)	0.876[a]
Female/total	10(25)	10(26)	0.45[c]
CDRS	41.36(17.13)	17.46(1.14)	p<0.0001[a]
HDRS	11(6)	0.5(1.03)	p<0.0001[a]
Hollingshead SES score	47.09(13.82)	44.48(13.70)	0.524[a]
Petersen pubertal development score	2.41(0.83)	2.39(0.94)	0.950[a]
Age of onset	10.12(2.37)	-	-
Education	1.6(0.5)	1.62(0.50)	0.913[a]
ADHD	10	-	-
Panic disorder	1	-	-
Social phobia	3	-	-
OCD	1	-	-
ODD	5	-	-
GAD	9	-	-
Enuresis	4	-	-
Encopresis	2	-	-
Drug abuse	1	-	-
SAD	9	-	-
Specific/simple phobia	2	-	-
Agoraphobia	2	-	-
Conduct disorder	1	-	-
Binge eating disorder	1	-	-
Currently or previously taken any psychotropic medication	12	-	-
Handedness (Left)	3	1	0.34[b]
White	11	6	0.14[b]
Black	2	1	0.61[b]
Hispanic	10	18	0.05[b]
Others	2	1	0.61[b]

[a] student t-test,

[b] Fisher's exact test,

[c] chi-square test,

PUD- pediatric unipolar depression, SD- standard deviation, OCD- obsessive compulsive disorder, ODD- opposition defiant disorder, GAD- generalized anxiety disorder, SAD – social anxiety disorder, ADHD- Attention deficit hyperactivity disorder, CDRS- child depression rating scale, HDRS- Hamilton depression rating scale, SES – social economic status.

Table 2

Neuromorphometric feature indices and prediction performance using SVM with 2nd order polynomial kernel

Feature	Accuracy	Sensitivity [95% Confidence interval]	Specificity [95% Confidence interval]	Chi-square P-value
Folding index	45.10%	24.00% [9.42%, 45.13%]	65.38% [44.34%, 82.75%]	0.4056
Intrinsic curvature index	66.67%	40.00% [21.16%, 61.32%]	92.31% [74.83%, 98.83%]	0.0065
Mean curvature	50.98%	32.00% [14.99%, 53.50%]	69.23% [48.21%, 85.63%.]	0.9246
Gaussian curvature	64.71%	44.00% [24.43%, 65.06%]	84.62% [65.11%, 95.55%]	0.025
Cortical surface area	17.65%	12.00% [2.69%, 31.25%]	23.08% [9.03%, 43.65%]	p < 0.005
Cortical thickness	52.94%	56.00% [34.94%, 75.57 %]	50.00% [29.94%, 70.06%]	0.6678
Subcortical volume	64.71%	64.00% [42.53%, 81.99%]	64.00% [44.34%, 82.75%]	0.0359
All features	78.43%	64.00% [54.87%, 90.58%]	80.77% [60.64%, 93.37%]	p < 0.005